

PDF hosted at the Radboud Repository of the Radboud University Nijmegen

The following full text is a preprint version which may differ from the publisher's version.

For additional information about this publication click this link.

<http://hdl.handle.net/2066/84060>

Please be advised that this information was generated on 2018-07-08 and may be subject to change.

Search for scalar bottom quarks and third-generation leptoquarks in $p\bar{p}$ collisions at $\sqrt{s} = 1.96$ TeV

V.M. Abazov,³⁶ B. Abbott,⁷⁴ M. Abolins,⁶³ B.S. Acharya,²⁹ M. Adams,⁴⁹ T. Adams,⁴⁷ E. Aguilo,⁶ G.D. Alexeev,³⁶ G. Alkhazov,⁴⁰ A. Alton^a,⁶² G. Alverson,⁶¹ G.A. Alves,² L.S. Ancu,³⁵ M. Aoki,⁴⁸ Y. Arnaud,¹⁴ M. Arov,⁵⁸ A. Askew,⁴⁷ B. Åsman,⁴¹ O. Atramentov,⁶⁶ C. Avila,⁸ J. BackusMayes,⁸¹ F. Badaud,¹³ L. Bagby,⁴⁸ B. Baldin,⁴⁸ D.V. Bandurin,⁴⁷ S. Banerjee,²⁹ E. Barberis,⁶¹ A.-F. Barfuss,¹⁵ P. Baringer,⁵⁶ J. Barreto,² J.F. Bartlett,⁴⁸ U. Bessler,¹⁸ S. Beale,⁶ A. Bean,⁵⁶ M. Begalli,³ M. Begel,⁷² C. Belanger-Champagne,⁴¹ L. Bellantoni,⁴⁸ J.A. Benitez,⁶³ S.B. Beri,²⁷ G. Bernardi,¹⁷ R. Bernhard,²² I. Bertram,⁴² M. Besançon,¹⁸ R. Beuselinck,⁴³ V.A. Bezzubov,³⁹ P.C. Bhat,⁴⁸ V. Bhatnagar,²⁷ G. Blazey,⁵⁰ S. Blessing,⁴⁷ K. Bloom,⁶⁵ A. Boehnlein,⁴⁸ D. Boline,⁷¹ T.A. Bolton,⁵⁷ E.E. Boos,³⁸ G. Borissov,⁴² T. Bose,⁶⁰ A. Brandt,⁷⁷ R. Brock,⁶³ G. Brooijmans,⁶⁹ A. Bross,⁴⁸ D. Brown,¹⁹ X.B. Bu,⁷ D. Buchholz,⁵¹ M. Buehler,⁸⁰ V. Buescher,²⁴ V. Bunichev,³⁸ S. Burdin,⁶⁴² T.H. Burnett,⁸¹ C.P. Buszello,⁴³ P. Calfayan,²⁵ B. Calpas,¹⁵ S. Calvet,¹⁶ E. Camacho-Pérez,³³ J. Cammin,⁷⁰ M.A. Carrasco-Lizarraga,³³ E. Carrera,⁴⁷ B.C.K. Casey,⁴⁸ H. Castilla-Valdez,³³ S. Chakrabarti,⁷¹ D. Chakraborty,⁵⁰ K.M. Chan,⁵⁴ A. Chandra,⁷⁹ G. Chen,⁵⁶ S. Chevalier-Théry,¹⁸ D.K. Cho,⁷⁶ S.W. Cho,³¹ S. Choi,³² B. Choudhary,²⁸ T. Christoudias,⁴³ S. Cihangir,⁴⁸ D. Claes,⁶⁵ J. Clutter,⁵⁶ M. Cooke,⁴⁸ W.E. Cooper,⁴⁸ M. Corcoran,⁷⁹ F. Couderc,¹⁸ M.-C. Cousinou,¹⁵ A. Croc,¹⁸ D. Cutts,⁷⁶ M. Cwiok,³⁰ A. Das,⁴⁵ G. Davies,⁴³ K. De,⁷⁷ S.J. de Jong,³⁵ E. De La Cruz-Burelo,³³ F. Déliot,¹⁸ M. Demarteau,⁴⁸ R. Demina,⁷⁰ D. Denisov,⁴⁸ S.P. Denisov,³⁹ S. Desai,⁴⁸ K. DeVaughan,⁶⁵ H.T. Diehl,⁴⁸ M. Diesburg,⁴⁸ A. Dominguez,⁶⁵ T. Dorland,⁸¹ A. Dubey,²⁸ L.V. Dudko,³⁸ D. Duggan,⁶⁶ A. Duperrin,¹⁵ S. Dutt,²⁷ A. Dyshkant,⁵⁰ M. Eads,⁶⁵ D. Edmunds,⁶³ J. Ellison,⁴⁶ V.D. Elvira,⁴⁸ Y. Enari,¹⁷ S. Eno,⁵⁹ H. Evans,⁵² A. Evdokimov,⁷² V.N. Evdokimov,³⁹ G. Facini,⁶¹ A.V. Ferapontov,⁷⁶ T. Ferbel,^{59,70} F. Fiedler,²⁴ F. Filthaut,³⁵ W. Fisher,⁶³ H.E. Fisk,⁴⁸ M. Fortner,⁵⁰ H. Fox,⁴² S. Fuess,⁴⁸ T. Gadfort,⁷² A. Garcia-Bellido,⁷⁰ V. Gavrilov,³⁷ P. Gay,¹³ W. Geist,¹⁹ W. Geng,^{15,63} D. Gerbaudo,⁶⁷ C.E. Gerber,⁴⁹ Y. Gershtein,⁶⁶ D. Gillberg,⁶ G. Ginter,^{48,70} G. Golovanov,³⁶ A. Goussiou,⁸¹ P.D. Grannis,⁷¹ S. Greder,¹⁹ H. Greenlee,⁴⁸ Z.D. Greenwood,⁵⁸ E.M. Gregores,⁴ G. Grenier,²⁰ Ph. Gris,¹³ J.-F. Grivaz,¹⁶ A. Grohsjean,¹⁸ S. Grünendahl,⁴⁸ M.W. Grünewald,³⁰ F. Guo,⁷¹ J. Guo,⁷¹ G. Gutierrez,⁴⁸ P. Gutierrez,⁷⁴ A. Haas^c,⁶⁹ P. Haefner,²⁵ S. Hagopian,⁴⁷ J. Haley,⁶¹ I. Hall,⁶³ L. Han,⁷ K. Harder,⁴⁴ A. Harel,⁷⁰ J.M. Hauptman,⁵⁵ J. Hays,⁴³ T. Hebbeker,²¹ D. Hedin,⁵⁰ A.P. Heinson,⁴⁶ U. Heintz,⁷⁶ C. Hensel,²³ I. Heredia-De La Cruz,³³ K. Herner,⁶² G. Hesketh,⁶¹ M.D. Hildreth,⁵⁴ R. Hirosky,⁸⁰ T. Hoang,⁴⁷ J.D. Hobbs,⁷¹ B. Hoeneisen,¹² M. Hohlfield,²⁴ S. Hossain,⁷⁴ P. Houben,³⁴ Y. Hu,⁷¹ Z. Hubacek,¹⁰ N. Huske,¹⁷ V. Hynek,¹⁰ I. Iashvili,⁶⁸ R. Illingworth,⁴⁸ A.S. Ito,⁴⁸ S. Jabeen,⁷⁶ M. Jaffré,¹⁶ S. Jain,⁶⁸ D. Jamin,¹⁵ R. Jesik,⁴³ K. Johns,⁴⁵ C. Johnson,⁶⁹ M. Johnson,⁴⁸ D. Johnston,⁶⁵ A. Jonckheere,⁴⁸ P. Jonsson,⁴³ A. Juste^d,⁴⁸ K. Kaadze,⁵⁷ E. Kajfasz,¹⁵ D. Karmanov,³⁸ P.A. Kasper,⁴⁸ I. Katsanos,⁶⁵ R. Kehoe,⁷⁸ S. Kermiche,¹⁵ N. Khalatyan,⁴⁸ A. Khanov,⁷⁵ A. Kharchilava,⁶⁸ Y.N. Kharzheev,³⁶ D. Khatidze,⁷⁶ M.H. Kirby,⁵¹ M. Kirsch,²¹ J.M. Kohli,²⁷ A.V. Kozelov,³⁹ J. Kraus,⁶³ A. Kumar,⁶⁸ A. Kupco,¹¹ T. Kurča,²⁰ V.A. Kuzmin,³⁸ J. Kvita,⁹ S. Lammers,⁵² G. Landsberg,⁷⁶ P. Lebrun,²⁰ H.S. Lee,³¹ W.M. Lee,⁴⁸ J. Lellouch,¹⁷ L. Li,⁴⁶ Q.Z. Li,⁴⁸ S.M. Lietti,⁵ J.K. Lim,³¹ D. Lincoln,⁴⁸ J. Linnemann,⁶³ V.V. Lipaev,³⁹ R. Lipton,⁴⁸ Y. Liu,⁷ Z. Liu,⁶ A. Lobodenko,⁴⁰ M. Lokajicek,¹¹ P. Love,⁴² H.J. Lubatti,⁸¹ R. Luna-Garcia^e,³³ A.L. Lyon,⁴⁸ A.K.A. Maciel,² D. Mackin,⁷⁹ R. Madar,¹⁸ R. Magaña-Villalba,³³ P.K. Mal,⁴⁵ S. Malik,⁶⁵ V.L. Malyshev,³⁶ Y. Maravin,⁵⁷ J. Martínez-Ortega,³³ R. McCarthy,⁷¹ C.L. McGivern,⁵⁶ M.M. Meijer,³⁵ A. Melnitchouk,⁶⁴ D. Menezes,⁵⁰ P.G. Mercadante,⁴ M. Merkin,³⁸ A. Meyer,²¹ J. Meyer,²³ N.K. Mondal,²⁹ T. Moulik,⁵⁶ G.S. Muanza,¹⁵ M. Mulhearn,⁸⁰ E. Nagy,¹⁵ M. Naimuddin,²⁸ M. Narain,⁷⁶ R. Nayyar,²⁸ H.A. Neal,⁶² J.P. Negret,⁸ P. Neustroev,⁴⁰ H. Nilsen,²² S.F. Novaes,⁵ T. Nunnemann,²⁵ G. Obrant,⁴⁰ D. Onoprienko,⁵⁷ J. Orduna,³³ N. Osman,⁴³ J. Osta,⁵⁴ G.J. Otero y Garzón,¹ M. Owen,⁴⁴ M. Padilla,⁴⁶ M. Pangilinan,⁷⁶ N. Parashar,⁵³ V. Parihar,⁷⁶ S.-J. Park,²³ S.K. Park,³¹ J. Parsons,⁶⁹ R. Partridge^c,⁷⁶ N. Parua,⁵² A. Patwa,⁷² B. Penning,⁴⁸ M. Perfilov,³⁸ K. Peters,⁴⁴ Y. Peters,⁴⁴ G. Petrillo,⁷⁰ P. Pétrouff,¹⁶ R. Piegai,¹ J. Piper,⁶³ M.-A. Pleier,⁷² P.L.M. Podesta-Lerma^f,³³ V.M. Podstavkov,⁴⁸ M.-E. Pol,² P. Polozov,³⁷ A.V. Popov,³⁹ M. Prewitt,⁷⁹ D. Price,⁵² S. Protopopescu,⁷² J. Qian,⁶² A. Quadt,²³ B. Quinn,⁶⁴ M.S. Rangel,¹⁶ K. Ranjan,²⁸ P.N. Ratoff,⁴² I. Razumov,³⁹ P. Renkel,⁷⁸ P. Rich,⁴⁴ M. Rijssenbeek,⁷¹ I. Ripp-Baudot,¹⁹ F. Rizatdinova,⁷⁵ M. Rominsky,⁴⁸ C. Royon,¹⁸ P. Rubinov,⁴⁸ R. Ruchti,⁵⁴ G. Safronov,³⁷ G. Sajot,¹⁴ A. Sánchez-Hernández,³³ M.P. Sanders,²⁵ B. Sanghi,⁴⁸ G. Savage,⁴⁸ L. Sawyer,⁵⁸ T. Scanlon,⁴³ D. Schaile,²⁵ R.D. Schamberger,⁷¹ Y. Scheglov,⁴⁰ H. Schellman,⁵¹ T. Schliephake,²⁶ S. Schlobohm,⁸¹ C. Schwanenberger,⁴⁴ R. Schwienhorst,⁶³ J. Sekaric,⁵⁶ H. Severini,⁷⁴ E. Shabalina,²³ V. Shary,¹⁸ A.A. Shchukin,³⁹ R.K. Shivpuri,²⁸ V. Simak,¹⁰ V. Sirotenko,⁴⁸ P. Skubic,⁷⁴ P. Slattery,⁷⁰ D. Smirnov,⁵⁴ G.R. Snow,⁶⁵ J. Snow,⁷³ S. Snyder,⁷² S. Söldner-Rembold,⁴⁴ L. Sonnenschein,²¹

A. Sopczak,⁴² M. Sosebee,⁷⁷ K. Soustruznik,⁹ B. Spurlock,⁷⁷ J. Stark,¹⁴ V. Stolin,³⁷ D.A. Stoyanova,³⁹
M.A. Strang,⁶⁸ E. Strauss,⁷¹ M. Strauss,⁷⁴ R. Ströhmer,²⁵ D. Strom,⁴⁹ L. Stutte,⁴⁸ P. Svoisky,³⁵ M. Takahashi,⁴⁴
A. Tanasijczuk,¹ W. Taylor,⁶ B. Tiller,²⁵ M. Titov,¹⁸ V.V. Tokmenin,³⁶ D. Tsybychev,⁷¹ B. Tuchming,¹⁸ C. Tully,⁶⁷
P.M. Tuts,⁶⁹ R. Unalan,⁶³ L. Uvarov,⁴⁰ S. Uvarov,⁴⁰ S. Uzunyan,⁵⁰ R. Van Kooten,⁵² W.M. van Leeuwen,³⁴
N. Varelas,⁴⁹ E.W. Varnes,⁴⁵ I.A. Vasilyev,³⁹ P. Verdier,²⁰ L.S. Vertogradov,³⁶ M. Verzocchi,⁴⁸ M. Vesterinen,⁴⁴
D. Vilanova,¹⁸ P. Vint,⁴³ P. Vokac,¹⁰ H.D. Wahl,⁴⁷ M.H.L.S. Wang,⁷⁰ J. Warchol,⁵⁴ G. Watts,⁸¹ M. Wayne,⁵⁴
G. Weber,²⁴ M. Weber,^{9, 48} M. Wetstein,⁵⁹ A. White,⁷⁷ D. Wicke,²⁴ M.R.J. Williams,⁴² G.W. Wilson,⁵⁶
S.J. Wimpenny,⁴⁶ M. Wobisch,⁵⁸ D.R. Wood,⁶¹ T.R. Wyatt,⁴⁴ Y. Xie,⁴⁸ C. Xu,⁶² S. Yacoob,⁵¹ R. Yamada,⁴⁸
W.-C. Yang,⁴⁴ T. Yasuda,⁴⁸ Y.A. Yatsunenko,³⁶ Z. Ye,⁴⁸ H. Yin,⁷ K. Yip,⁷² H.D. Yoo,⁷⁶ S.W. Youn,⁴⁸
J. Yu,⁷⁷ S. Zelitch,⁸⁰ T. Zhao,⁸¹ B. Zhou,⁶² J. Zhu,⁷¹ M. Zielinski,⁷⁰ D. Zieminska,⁵² and L. Zivkovic⁶⁹

(The D0 Collaboration*)

¹Universidad de Buenos Aires, Buenos Aires, Argentina

²LAFEX, Centro Brasileiro de Pesquisas Físicas, Rio de Janeiro, Brazil

³Universidade do Estado do Rio de Janeiro, Rio de Janeiro, Brazil

⁴Universidade Federal do ABC, Santo André, Brazil

⁵Instituto de Física Teórica, Universidade Estadual Paulista, São Paulo, Brazil

⁶Simon Fraser University, Vancouver, British Columbia, and York University, Toronto, Ontario, Canada

⁷University of Science and Technology of China, Hefei, People's Republic of China

⁸Universidad de los Andes, Bogotá, Colombia

⁹Charles University, Faculty of Mathematics and Physics,
Center for Particle Physics, Prague, Czech Republic

¹⁰Czech Technical University in Prague, Prague, Czech Republic

¹¹Center for Particle Physics, Institute of Physics,
Academy of Sciences of the Czech Republic, Prague, Czech Republic

¹²Universidad San Francisco de Quito, Quito, Ecuador

¹³LPC, Université Blaise Pascal, CNRS/IN2P3, Clermont, France

¹⁴LPSC, Université Joseph Fourier Grenoble 1, CNRS/IN2P3,
Institut National Polytechnique de Grenoble, Grenoble, France

¹⁵CPPM, Aix-Marseille Université, CNRS/IN2P3, Marseille, France

¹⁶LAL, Université Paris-Sud, CNRS/IN2P3, Orsay, France

¹⁷LPNHE, Universités Paris VI and VII, CNRS/IN2P3, Paris, France

¹⁸CEA, Irfu, SPP, Saclay, France

¹⁹IPHC, Université de Strasbourg, CNRS/IN2P3, Strasbourg, France

²⁰IPNL, Université Lyon 1, CNRS/IN2P3, Villeurbanne, France and Université de Lyon, Lyon, France

²¹III. Physikalisches Institut A, RWTH Aachen University, Aachen, Germany

²²Physikalisches Institut, Universität Freiburg, Freiburg, Germany

²³II. Physikalisches Institut, Georg-August-Universität Göttingen, Göttingen, Germany

²⁴Institut für Physik, Universität Mainz, Mainz, Germany

²⁵Ludwig-Maximilians-Universität München, München, Germany

²⁶Fachbereich Physik, Bergische Universität Wuppertal, Wuppertal, Germany

²⁷Panjab University, Chandigarh, India

²⁸Delhi University, Delhi, India

²⁹Tata Institute of Fundamental Research, Mumbai, India

³⁰University College Dublin, Dublin, Ireland

³¹Korea Detector Laboratory, Korea University, Seoul, Korea

³²SungKyunKwan University, Suwon, Korea

³³CINVESTAV, Mexico City, Mexico

³⁴FOM-Institute NIKHEF and University of Amsterdam/NIKHEF, Amsterdam, The Netherlands

³⁵Radboud University Nijmegen/NIKHEF, Nijmegen, The Netherlands

³⁶Joint Institute for Nuclear Research, Dubna, Russia

³⁷Institute for Theoretical and Experimental Physics, Moscow, Russia

³⁸Moscow State University, Moscow, Russia

³⁹Institute for High Energy Physics, Protvino, Russia

⁴⁰Petersburg Nuclear Physics Institute, St. Petersburg, Russia

⁴¹Stockholm University, Stockholm and Uppsala University, Uppsala, Sweden

⁴²Lancaster University, Lancaster LA1 4YB, United Kingdom

⁴³Imperial College London, London SW7 2AZ, United Kingdom

⁴⁴The University of Manchester, Manchester M13 9PL, United Kingdom

⁴⁵University of Arizona, Tucson, Arizona 85721, USA

⁴⁶University of California Riverside, Riverside, California 92521, USA

⁴⁷Florida State University, Tallahassee, Florida 32306, USA

- ⁴⁸Fermi National Accelerator Laboratory, Batavia, Illinois 60510, USA
⁴⁹University of Illinois at Chicago, Chicago, Illinois 60607, USA
⁵⁰Northern Illinois University, DeKalb, Illinois 60115, USA
⁵¹Northwestern University, Evanston, Illinois 60208, USA
⁵²Indiana University, Bloomington, Indiana 47405, USA
⁵³Purdue University Calumet, Hammond, Indiana 46323, USA
⁵⁴University of Notre Dame, Notre Dame, Indiana 46556, USA
⁵⁵Iowa State University, Ames, Iowa 50011, USA
⁵⁶University of Kansas, Lawrence, Kansas 66045, USA
⁵⁷Kansas State University, Manhattan, Kansas 66506, USA
⁵⁸Louisiana Tech University, Ruston, Louisiana 71272, USA
⁵⁹University of Maryland, College Park, Maryland 20742, USA
⁶⁰Boston University, Boston, Massachusetts 02215, USA
⁶¹Northeastern University, Boston, Massachusetts 02115, USA
⁶²University of Michigan, Ann Arbor, Michigan 48109, USA
⁶³Michigan State University, East Lansing, Michigan 48824, USA
⁶⁴University of Mississippi, University, Mississippi 38677, USA
⁶⁵University of Nebraska, Lincoln, Nebraska 68588, USA
⁶⁶Rutgers University, Piscataway, New Jersey 08855, USA
⁶⁷Princeton University, Princeton, New Jersey 08544, USA
⁶⁸State University of New York, Buffalo, New York 14260, USA
⁶⁹Columbia University, New York, New York 10027, USA
⁷⁰University of Rochester, Rochester, New York 14627, USA
⁷¹State University of New York, Stony Brook, New York 11794, USA
⁷²Brookhaven National Laboratory, Upton, New York 11973, USA
⁷³Langston University, Langston, Oklahoma 73050, USA
⁷⁴University of Oklahoma, Norman, Oklahoma 73019, USA
⁷⁵Oklahoma State University, Stillwater, Oklahoma 74078, USA
⁷⁶Brown University, Providence, Rhode Island 02912, USA
⁷⁷University of Texas, Arlington, Texas 76019, USA
⁷⁸Southern Methodist University, Dallas, Texas 75275, USA
⁷⁹Rice University, Houston, Texas 77005, USA
⁸⁰University of Virginia, Charlottesville, Virginia 22901, USA
⁸¹University of Washington, Seattle, Washington 98195, USA

(Dated: May 12, 2010)

We report the results of a search for pair production of scalar bottom quarks (\tilde{b}_1) and scalar third-generation leptoquarks (LQ_3) in 5.2 fb^{-1} of $p\bar{p}$ collisions at the D0 experiment of the Fermilab Tevatron Collider. Scalar bottom quarks are assumed to decay to a neutralino ($\tilde{\chi}_1^0$) and a b quark, and we set 95% C.L. lower limits on their production in the $(m_{\tilde{b}_1}, m_{\tilde{\chi}_1^0})$ mass plane such as $m_{\tilde{b}_1} > 247 \text{ GeV}$ for $m_{\tilde{\chi}_1^0} = 0$ and $m_{\tilde{\chi}_1^0} > 110 \text{ GeV}$ for $160 < m_{\tilde{b}_1} < 200 \text{ GeV}$. The leptoquarks are assumed to decay to a tau neutrino and a b quark, and we set a 95% C.L. lower limit of 247 GeV on the mass of a charge-1/3 third-generation scalar leptoquark.

PACS numbers: 14.80.-j, 13.85.Rm

The standard model (SM) offers an accurate description of current experimental data in high energy physics but it is believed to be embedded in a more general theory. In particular, extensions of the SM to higher mass scales have been proposed that predict the existence of new particles and phenomena which can be searched for at the Tevatron.

Supersymmetric (SUSY) models provide an extension of the SM that resolves the ‘‘hierarchy problem’’ by introducing supersymmetric partners to the known fermions and bosons [1]. The supersymmetric quarks (squarks) are mixtures of the states \tilde{q}_L and \tilde{q}_R , the superpartners of the SM quark helicity states. The theory permits a mass difference between the squark mass eigenstates, \tilde{q}_1 and \tilde{q}_2 , and allows the possibility that the lighter states of top and bottom squarks have masses smaller than the squarks of the first two generations. In this analysis we consider the region of SUSY parameter space where the only decay of the lighter bottom squark is $\tilde{b}_1 \rightarrow b\tilde{\chi}_1^0$, with $m_b + m_{\tilde{\chi}_1^0} < m_{\tilde{b}_1} < m_t + m_{\tilde{\chi}_1^-}$, and the neutralino $\tilde{\chi}_1^0$ and chargino $\tilde{\chi}_1^\pm$ are the lightest SUSY partners of the electroweak and Higgs bosons. This analysis is inter-

*with visitors from ^aAugustana College, Sioux Falls, SD, USA, ^bThe University of Liverpool, Liverpool, UK, ^cSLAC, Menlo Park, CA, USA, ^dICREA/IFAE, Barcelona, Spain, ^eCentro de Investigacion en Computacion - IPN, Mexico City, Mexico, ^fECFM, Universidad Autonoma de Sinaloa, Culiacán, Mexico, and ^gUniversität Bern, Bern, Switzerland.

preted within the framework of the minimal supersymmetric standard model (MSSM) with R -parity [2] conservation, and under the hypothesis that the lightest, and consequently stable, SUSY particle is the $\tilde{\chi}_1^0$. We therefore search for $p\bar{p} \rightarrow \tilde{b}_1\tilde{b}_1 \rightarrow b\tilde{\chi}_1^0\bar{b}\tilde{\chi}_1^0$.

Leptoquarks are hypothesized fundamental particles that have color, electric charge, and both lepton and baryon quantum numbers. They appear in many extensions of the SM including extended gauge theories, composite models, and SUSY with R -parity violation [3]. Current models suggest that leptoquarks of each of the three generations should decay to the corresponding generation of SM leptons and quarks to avoid introducing unwanted flavor changing neutral currents. Charge-1/3 third-generation leptoquarks would decay to $b\nu$ with branching fraction B or to $t\tau$ with branching fraction $1 - B$.

We report on a search for the production of pairs of bottom squarks and third-generation scalar leptoquarks in data collected by the D0 Collaboration at the Fermilab Tevatron Collider. For both searches, the signature is defined to be two b -jets and missing transverse energy (\cancel{E}_T) from the escaping neutrinos or neutralinos. This topology is identical to that for $p\bar{p} \rightarrow ZH \rightarrow \nu\bar{\nu} + b\bar{b}$ production, and the two analyses are based on the same data and selection criteria [4]. Bottom squark or leptoquark pairs are expected to be produced mainly through $q\bar{q}$ annihilation or gg fusion, with identical leading order QCD production cross sections. We use the next-to-leading order (NLO) cross sections calculated by PROSPINO 2.1 for both bottom squark [5] and leptoquark [6] pair production, and found them to agree to better than 3%. Previous measurements excluded bottom squark masses $m_{\tilde{b}_1} < 222$ GeV for a massless neutralino [7], as well as charge-1/3 third-generation scalar leptoquark masses $m_{LQ} < 229$ GeV for $B = 1$ [8].

The D0 detector [9] consists of layered systems surrounding the interaction point. The momenta of charged particles and the location of the interaction vertices are determined using a silicon microstrip tracker and a central fiber tracker immersed in the magnetic field of a 2 T solenoid. Jets, electrons, and tau leptons are reconstructed using the tracking information and the pattern of energy deposits in three uranium/liquid-argon calorimeters located outside the tracking system with a central calorimeter covering pseudorapidity $|\eta| < 1.1$, and two end calorimeters housed in separate cryostats covering the regions up to $|\eta| \approx 4.2$. Jet reconstruction uses a cone algorithm [10] with radius $\mathcal{R} = \sqrt{(\Delta y)^2 + (\Delta\phi)^2} = 0.5$ in rapidity (y) and azimuth (ϕ). Muons are identified through the association of tracks with hits in the muon system, which is outside of the calorimeter and consists of drift tubes and scintillation counters before and after 1.8 T iron toroids. The \cancel{E}_T is determined from the negative of the vector sum of the transverse components of the energy deposited in the calorimeter and the transverse momenta p_T of detected muons. The jet energies are calibrated using transverse

energy balance in events with photons and jets and this calibration is propagated to the value of \cancel{E}_T .

The data were recorded using triggers based on jets and the \cancel{E}_T in the event. In addition to requirements on \cancel{E}_T and jet energy, the vector sum of the transverse energies of all jets, defined as $\cancel{H}_T \equiv |\sum_{\text{jets}} \vec{p}_T|$, the scalar sum of the p_T of the jets (H_T), and the angle α between the two leading jets in the transverse plane, are also used for triggering. Typical requirements are $\cancel{E}_T > 25$ GeV, $\cancel{H}_T > 25$ GeV, $H_T > 50$ GeV, and $\alpha < 169^\circ$. After imposing quality requirements, the data correspond to an integrated luminosity of 5.2 fb^{-1} . The previous D0 publications [7, 8] used a subset of this data sample, and are superseded by the results obtained in this Letter.

Monte Carlo (MC) samples for $200 < m_{LQ} < 280$ GeV, and for $(\tilde{b}_1, \tilde{\chi}_1^0)$ pairs with $80 < m_{\tilde{b}_1} < 260$ GeV and $m_{\tilde{\chi}_1^0} < 120$ GeV, are generated with PYTHIA [11]. Backgrounds from SM processes with significant \cancel{E}_T are estimated using MC. The most important backgrounds are from W/Z bosons produced in association with jets, with leptonic decays such as $Z \rightarrow \nu\bar{\nu}$ and $W \rightarrow e\nu$, and processes with $t\bar{t}$ and single top quark production. The cross sections used to estimate these contributions to the background are obtained from [12] and [13]. At the parton level, vector boson pair production and the single-top quark events are generated with PYTHIA and COMPHEP [14], respectively, while ALPGEN [15] is used for all other samples. All MC events are then processed with PYTHIA, which performs parton showering and hadronization. The resulting samples are processed using a GEANT [16] simulation of the D0 detector. To model the effects of multiple interactions and detector noise, data from random $p\bar{p}$ crossings are overlaid on MC events. The CTEQ6L1 parameterization [17] is used for all parton density functions (PDF). Instrumental background comes mostly from multijet processes with \cancel{E}_T arising from energy mismeasurement. This background, which we label MJ, dominates the low \cancel{E}_T region and is modeled using data.

A signal sample and a sample used to model the MJ background are selected. We select events with two or three jets with $|\eta| < 2.5$ and $p_T > 20$ GeV, and require that the interaction vertex has at least three tracks and is reconstructed within ± 40 cm of the center of the detector along the beam direction so that the tracks are within the geometric acceptance of the silicon tracker. As the leading highest p_T jets in the signal events are assumed to originate from decays of b quarks, we require that at least two jets, including the leading jet, have at least two tracks pointing to the primary vertex in order to apply b -tagging algorithms. We also require the two leading jets satisfy $\alpha < 165^\circ$. To reduce the contribution from $W \rightarrow l\nu$ decays, we veto events with isolated electrons or muons with $p_T > 15$ GeV, as well as tau leptons that decay hadronically to a single charged particle with $p_T > 12$ GeV when there is no associated electromagnetic cluster or $p_T > 10$ GeV if there is such a cluster [18]. To suppress the MJ background, we require $\cancel{E}_T > 40$ GeV

and \cancel{E}_T significance $\mathcal{S} > 5$ [19]. We also remove events when the direction of the \cancel{E}_T overlaps with a jet in ϕ by requiring $\cancel{E}_T/\text{GeV} > 80 - 40 \times \Delta\phi_{\min}(\cancel{E}_T, \text{jets})$, where $\Delta\phi_{\min}(\cancel{E}_T, \text{jets})$ denotes the minimum of the angles between the \cancel{E}_T and any of the selected jets.

The contribution from multijet processes is determined using the techniques described in [4]. For signal events, the direction of \cancel{E}_T tends to be aligned with the missing track transverse momentum, \cancel{p}_T , defined as the negative of the vectorial sum of the p_T of the charged particles. A strong correlation of this kind is not expected in multijet events, where \cancel{E}_T originates mainly from mismeasurement of jet energies in the calorimeter. We exploit this difference by requiring $\mathcal{D} < \pi/2$ for signal, where \mathcal{D} is the azimuthal distance between \cancel{E}_T and \cancel{p}_T , $\Delta\phi(\cancel{E}_T, \cancel{p}_T)$, and use events with $\mathcal{D} > \pi/2$ to model the kinematic distributions of the MJ background in the signal sample after subtracting the contribution from SM processes. The MJ background is normalized before b -tagging by requiring the number of observed events in data to equal the sum of SM and MJ contributions in the $\mathcal{D} < \pi/2$ region. The signal contribution is assumed to be zero. Figure 1 shows the \cancel{E}_T distribution and the background contributions from SM and MJ sources after these selections.

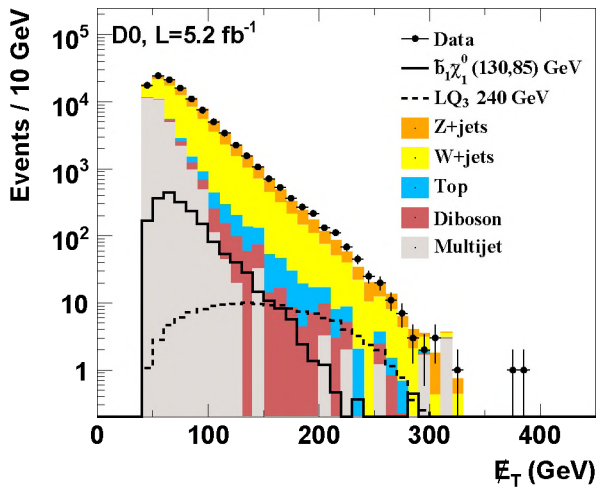


FIG. 1: (color online). The \cancel{E}_T distribution before b -tagging. The points with the error bars represent data while the shaded histograms show the contributions from background processes. Signal distributions with $(m_{\tilde{b}_1}, m_{\tilde{\chi}_1^0}) = (130, 85)$ GeV and $m_{LQ} = 240$ GeV are shown as solid and dashed lines, respectively.

A neural network (NN) b -tagging algorithm [20] is used to identify heavy-flavor jets, and reduce the SM and MJ backgrounds that are dominated by light flavor jets. We apply b -tagging and use the requirements on the NN output that give one jet to be tagged with an average efficiency of $\approx 70\%$ and the other with an average efficiency of $\approx 50\%$, where the corresponding probabilities of a light-

flavored jet to be wrongly identified as a b -jet are $\approx 6.5\%$ and $\approx 0.5\%$, respectively. These conditions are designed to optimize the discovery reach for a \tilde{b}_1 and LQ_3 .

Additional selections reduce the remaining number of events with poorly measured \cancel{E}_T . We require $\Delta\phi_{\min}(\cancel{E}_T, \text{jets}) > 0.6$ rad, and define an asymmetry $\mathcal{A} = (\cancel{E}_T - \cancel{H}_T)/(\cancel{E}_T + \cancel{H}_T)$ and require $-0.1 < \mathcal{A} < 0.2$ [21]. The \cancel{E}_T and H_T distributions after imposing b -tagging and the requirements on $\Delta\phi_{\min}(\cancel{E}_T, \text{jets})$ and \mathcal{A} are shown in Fig. 2, along with the expectations for two possible signals which show the kinematic variation for different masses.

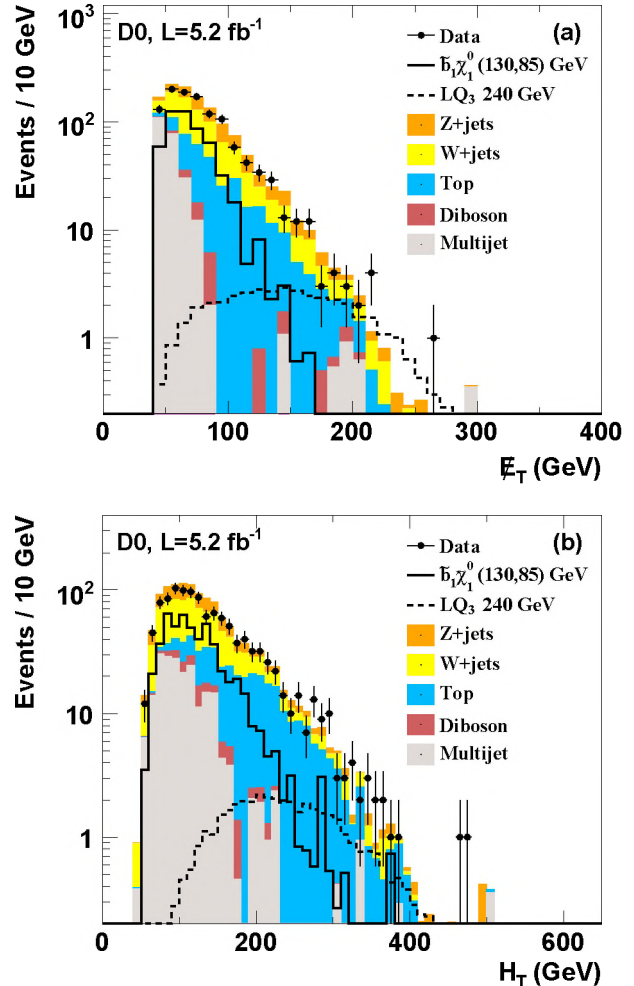


FIG. 2: (color online). The (a) \cancel{E}_T and (b) H_T distributions after b -tagging and additional selections. The points with the error bars represent data while the shaded histograms show the contributions from background processes. Signal distributions with $(m_{\tilde{b}_1}, m_{\tilde{\chi}_1^0}) = (130, 85)$ GeV and $m_{LQ} = 240$ GeV are shown as solid and dashed lines, respectively

We then apply final selections to improve the sensitivity. As our signals consist of two high- p_T b -jets, we use $X_{jj} \equiv (p_T^{\text{jet1}} + p_T^{\text{jet2}})/H_T$ as a discriminant against top-quark processes. We optimize selections on p_T^{jet1} , \cancel{E}_T ,

TABLE I: Predicted and observed numbers of events before and after b -tagging and additional event selections. The number of background events after pretag selection is normalized to the number of data events. Signal acceptances and the predicted number of events are given for two $(m_{\tilde{b}_1}, m_{\tilde{\chi}_1^0})$ mass points. The acceptances for $m_{LQ} = 240$ GeV and $(m_{\tilde{b}_1}, m_{\tilde{\chi}_1^0}) = (240, 0)$ GeV are identical. The uncertainties on the total background and the signals include all statistical and systematic uncertainties.

Process	Pretag	b -tag	$-0.1 < \mathcal{A} < 0.2$ $\Delta\phi(\cancel{E}_T, \text{jets}) > 0.6$	$X_{jj} > 0.75$ $p_T^{\text{jet1}} > 20$ GeV $\cancel{E}_T > 40$ GeV $H_T > 60$ GeV	$X_{jj} > 0.9$ $p_T^{\text{jet1}} > 50$ GeV $\cancel{E}_T > 150$ GeV $H_T > 220$ GeV
Diboson	2,060	38	35	31	0.3
$W(\rightarrow l\nu) + \text{light jets}$	49,250	130	119	105	0.5
$Wc\bar{c}, Wb\bar{b}$	7,792	353	325	261	1.9
$Z(\rightarrow ll) + \text{light jets}$	17,663	11	9	8	0
$Zc\bar{c}, Zb\bar{b}$	4,526	256	247	217	1.9
Top	2,019	348	301	190	2.2
MJ	30,243	444	205	157	0
Total background	113,553	$1,579 \pm 230$	$1,242 \pm 188$	971 ± 152	6.9 ± 1.7
# data events	113,553	1,463	1,131	901	7
Signal (acceptance, %)					
$(m_{\tilde{b}_1}, m_{\tilde{\chi}_1^0}) = (240, 0)$ GeV	145 ± 11 (38.7)	43.3 ± 6.4 (11.4)	42.0 ± 6.2 (11.1)	-	10.5 ± 1.9 (2.8)
$(m_{\tilde{b}_1}, m_{\tilde{\chi}_1^0}) = (130, 85)$ GeV	$1,928 \pm 158$ (10.9)	544 ± 85 (3.1)	529 ± 77 (3.0)	481 ± 66 (2.7)	-

H_T , and X_{jj} for different $(m_{\tilde{b}_1}, m_{\tilde{\chi}_1^0})$ and m_{LQ} by choosing selections that yield the smallest expected limit on the cross section. These selections are more restrictive for LQ_3 and \tilde{b}_1 signals with larger mass. For regions with small $m_{\tilde{b}_1} - m_{\tilde{\chi}_1^0}$, the average \cancel{E}_T and jet energies are lower, and relaxed requirements are found to be optimal. The results of the selections, and the predicted numbers of events from background processes are listed in Table I, including two final signal selection examples. For a signal with high \cancel{E}_T , the largest backgrounds are from $W/Z + b\bar{b}$ production and top quark processes. There is in addition a significant contribution from multijets for bottom squark signal points with a small value of \cancel{E}_T .

Systematic uncertainties include those on the integrated luminosity (6.1%), trigger efficiency (2%), and jet energy calibration and reconstruction (3% for signal and (2–7)% for background). Uncertainties associated with b -tagging are (6–17)% for signal and (5–11)% for background. Uncertainties on theoretical cross sections for SM processes include 10% on top quark production, and 6% on the total $(W/Z)+\text{jets}$ cross section with an additional 20% uncertainty on heavy flavor content. The contribution from the MJ background is assigned a 25% uncertainty which includes the impact of possible signal events contained in the pretag sample.

We obtain limits on the pair production cross section multiplied by the branching fraction squared ($\sigma \times B^2$) using the CL_s approach [22]. In this technique, an ensemble of MC experiments using the expected numbers of signal and background events is compared to the number of events observed in data to derive an exclusion limit. Signal and background contributions are varied within their uncertainties taking into account correlations among their systematic uncertainties. The LQ_3 and \tilde{b}_1 ($m_{\tilde{\chi}_1^0} = 0$) observed and expected cross section

limits are given in Table II.

TABLE II: Observed and expected 95% C.L. limits on the cross section for different leptoquark or bottom squark (assuming $m_{\tilde{\chi}_1^0} = 0$) masses.

Mass (GeV)	220	240	250	260	280
Observed (pb)	0.077	0.063	0.056	0.052	0.054
Expected (pb)	0.067	0.056	0.049	0.046	0.040

Figure 3(a) shows the 95% C.L. upper limits on the cross section as a function of m_{LQ} , together with the theoretical cross section σ_{th} assuming $B = 1$. The uncertainty on σ_{th} is obtained by varying the renormalization and factorization scales by a factor of two from the nominal choice $\mu = m_{LQ}$ and incorporating the PDF uncertainties [6]. Limits on m_{LQ} are obtained from the intersection of the observed cross section limit with the central σ_{th} and yield a lower mass limit of 247 GeV for $B = 1$ for the production of third-generation leptoquarks. If the 95% C.L. experimental limit is compared with the one standard deviation lower value of σ_{th} , we obtain a mass limit of $m_{LQ} = 238$ GeV. Also shown is the central value of σ_{th} when the coupling to the $b\nu$ and $t\tau$ channels are identical, yielding $B = 1 - 0.5 \times F_{sp}$ where F_{sp} is a phase space suppression factor for the τt channel [8]. The mass limit in this case is 234 GeV.

Figure 3(b) shows the excluded region in the plane of the bottom squark versus neutralino mass obtained using the central σ_{th} . For $m_{\tilde{\chi}_1^0} = 0$, the limit is $m_{\tilde{b}_1} > 247$ GeV. The exclusion region extends to $m_{\tilde{\chi}_1^0} = 110$ GeV for $160 < m_{\tilde{b}_1} < 200$ GeV.

In conclusion, in the 5.2 fb^{-1} data sample studied, the observed number of events with the topology of two b -jets plus missing transverse energy is consistent with that

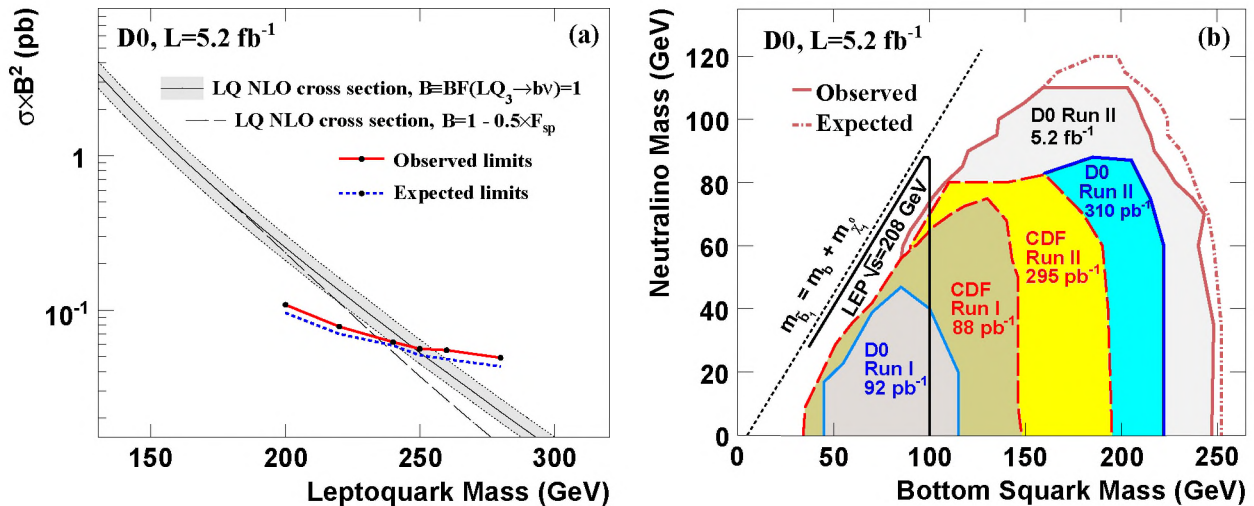


FIG. 3: (color online). (a) The 95% C.L. expected (dashed line) and observed (points plus solid line) limits on $\sigma \times B^2$ as a function of m_{LQ} for the pair production of third-generation leptoquarks where B is the branching fraction to $b\nu$. The theory band is shown in grey with an uncertainty range as discussed in the text. The long-dashed line indicates the expected suppression of $\sigma \times B^2$ above the $t\tau$ threshold for equal $b\nu$ and $t\tau$ couplings. (b) The 95% C.L. exclusion contour in the $(m_{\tilde{b}_1}, m_{\tilde{\chi}_1^0})$ plane. Also shown are results from previous searches at LEP [23] and the Tevatron [7, 24].

expected from known SM processes. We set limits on the cross section multiplied by square of the branching fraction B to the $b\nu$ final state as a function of leptoquark mass. These results are interpreted as mass limits and give a limit of 247 GeV for $B = 1$ for the production of charge-1/3 third-generation scalar leptoquarks. We also exclude the production of bottom squarks for a range of values in the $(m_{\tilde{b}_1}, m_{\tilde{\chi}_1^0})$ mass plane such as $m_{\tilde{b}_1} > 247$ GeV for $m_{\tilde{\chi}_1^0} = 0$ and $m_{\tilde{\chi}_1^0} > 110$ GeV for $160 < m_{\tilde{b}_1} < 200$ GeV. These limits significantly extend previous results.

We thank the staffs at Fermilab and collaborating

institutions, and acknowledge support from the DOE and NSF (USA); CEA and CNRS/IN2P3 (France); FASI, Rosatom and RFBR (Russia); CNPq, FAPERJ, FAPESP and FUNDUNESP (Brazil); DAE and DST (India); Colciencias (Colombia); CONACyT (Mexico); KRF and KOSEF (Korea); CONICET and UBACyT (Argentina); FOM (The Netherlands); STFC and the Royal Society (United Kingdom); MSMT and GACR (Czech Republic); CRC Program and NSERC (Canada); BMBF and DFG (Germany); SFI (Ireland); The Swedish Research Council (Sweden); and CAS and CNSF (China).

-
- [1] H.E. Haber and G.L. Kane, Phys. Rep. **117**, 75 (1985); S. P. Martin, arXiv:hep-ph/9709356 and references therein.
 [2] P. Fayet, Phys. Rev. Lett. **69**, 489 (1977).
 [3] D. E. Acosta and S. K. Blessing, Ann. Rev. Nucl. Part. Sci. **49**, 389 (1999) and references therein; C. Amsler *et al.*, Phys. Lett. B **667**, 1 (2008).
 [4] V.M. Abazov *et al.* (D0 Collaboration), Phys. Rev. Lett. **104**, 071801 (2010).
 [5] W. Beenaakker *et al.*, Nucl. Phys. **B515**, 3 (1998); www.thphys.uni-heidelberg.de/~plehn/prospino/. The calculation used a gluino mass of 609 GeV.
 [6] M. Kramer, T. Plehn, M. Spira, and P. M. Zerwas, Phys. Rev. Lett. **79**, 341 (1997).
 [7] V.M. Abazov *et al.* (D0 Collaboration), Phys. Rev. Lett. **97**, 171806 (2006); V.M. Abazov *et al.* (D0 Collaboration), Phys. Rev. D **60**, R031101 (1999).
 [8] V.M. Abazov *et al.* (D0 Collaboration), Phys. Rev. Lett. **99**, 061801 (2007). Charge-2/3 and 4/3 third-generation leptoquarks have been excluded for $m_{LQ} < 210$ GeV assuming a 100% branching fraction into the $b\tau$ mode, V.M. Abazov *et al.* (D0 Collaboration), Phys. Rev. Lett. **101**, 241802 (2008).
 [9] V.M. Abazov *et al.* (D0 Collaboration), Nucl. Instrum. Methods in Phys. Res. A **565**, 463 (2006); M. Abolins *et al.*, Nucl. Instrum. Methods in Phys. Res. A **584**, 75 (2008); R. Angstadt *et al.*, arXiv.org:0911.2522 [phys.ins-det], submitted to Nucl. Instrum. Methods in Phys. Res. A.
 [10] G.C. Blazey *et al.*, arXiv:hep-ex/0005012.
 [11] T. Sjöstrand, S. Mrenna, and P. Skands, J. High Energy Phys. **05**, 026 (2006). We use version 6.323.
 [12] J.M. Campbell and R.K. Ellis, Phys.Rev. D **60**, 113006 (1999); J.M. Campbell and R.K. Ellis, Phys.Rev. D **62**, 114012 (2000).
 [13] M. Cacciari *et al.*, J. High Energy Phys. **4**, 068 (2004); N. Kidonakis and R. Vogt, Phys. Rev. D **68**, 114014

- (2003); N. Kidonakis, Phys. Rev. D **74**, 114012 (2006).
- [14] E. Boos *et al.* (CompHEP Collaboration), Nucl. Instrum. Methods in Phys. Res. A **534**, 250 (2004). We use version 4.4.
- [15] M.L. Mangano *et al.*, J. High Energy Phys. **07**, 001 (2003). We use version 2.13.
- [16] R. Brun and F. Carminati, CERN Program Library Long Writeup W5013, 1993 (unpublished).
- [17] J. Pumplin *et al.*, J. High Energy Phys. **07**, 012 (2002); D. Stump *et al.*, J. High Energy Phys. **10**, 046 (2003).
- [18] V.M. Abazov *et al.* (D0 Collaboration), Phys. Rev. Lett. **102**, 251801 (2009).
- [19] A. Schwartzman, Ph.D. thesis, Universidad de Buenos Aires, FERMILAB-THESIS-2004-21 (2004). Larger values of S correspond to E_T values that are less likely to be caused by fluctuations in jet energies.
- [20] V.M. Abazov *et al.* (D0 Collaboration), Nucl. Instrum. Methods in Phys. Res. A **620**, 490 (2010).
- [21] V.M. Abazov *et al.* (D0 Collaboration), Phys. Rev. Lett. **97**, 161803 (2006).
- [22] T. Junk, Nucl. Instrum. Methods in Phys. Res. A **434**, 435 (1999); A. Read, J. Phys. G **28**, 2693 (2002).
- [23] LEPSUSYWG: ALEPH, DELPHI, L3, and OPAL Collaborations, <http://lepsusy.web.cern.ch/lepsusy>, Report No. LEPSUSYWG/04-02.1.
- [24] T. Aaltonen *et al.* (CDF Collaboration), Phys. Rev. Lett. **76**, 072010 (2007); T. Affolder *et al.* (CDF Collaboration), Phys. Rev. Lett. **84**, 5704 (2000). T. Aaltonen *et al.* (CDF Collaboration), Phys. Rev. Lett. **105**, 081802 (2010).